(NASA-TM-85058) THERMALLY INDUCED SPIN RATE RIPPLE ON SPACECRAFT WITH LONG RADIAL APPENDAGES (NASA) 29 p HC A03/MF A01 CSCL 22B

N84-16249

Unclas
G3/18 18263

NASA

Technical Memorandum 85058

Thermally Induced Spin Rate Ripple on Spacecraft with Long Radial Appendages

Joseph V. Fedor

AUGUST 1983

National Aeronautics and
Space Administration

Goddard Space Flight Center
Greenbelt, Maryland 20771

TM 85058

THERMALLY INDUCED SPIN RATE RIPPLE ON SPACECRAFT WITH LONG RADIAL APPENDAGES

Joseph V. Fedor

August 1983

GODDARD SPACE FLIGHT CENTER
Greenbelt, Maryland

THERMALLY INDUCED SPIN RATE RIPPLE ON SPACECRAFT WITH LONG RADIAL APPENDAGES

Joseph V. Fedor

ABSTRACT

A thermally induced spin rate ripple hypothesis is proposed to explain the spin rate anomaly observed on ISEE-B (launched October 22, 1977). This involves the two radial 14.5 meter beryllium copper tape ribbons going in and out of the spacecraft hub shadow. A thermal lag time constant is applied to the thermally induced ribbon displacements which perturb the spin rate. It is inferred that the averaged thermally induced ribbon displacements are coupled to the ribbon angular motion. Qualitative analytic results show a possible exponential build up of the inplane motion of the ribbon which in turn causes the spin rate ripple, ultimately limited by damping in the ribbon and spacecraft. Qualitative increase in the oscillation period is also indicated and that the thermal lag is fundamental for the period increase. Numerical parameter values required to agree with in-orbit initial exponential build up (after a torquing maneuver) are found to be reasonable; those required for the ripple period are somewhat extreme.

CONTENTS

ILLUSTRATIONS

PRECEDING PAGE BLANK NOT FILMED

THERMALLY INDUCED SPIN RATE RIPPLE ON SPACECRAFT WITH LONG RADIAL APPENDAGES

1. INTRODUCTION

On October 22, 1977 the ISEE-B spacecraft, which is part of an international program between NASA and ESA, was launched into a highly eccentric earth orbit. After all spacecraft appendages were deployed and time had elapsed to damp out deployment transients, a disconcerting phenomenon was noted in the spin rate. There appeared to be sustained spin period fluctuations. Attempts were made to eliminate the spin rate ripple with on-board thruster and ground timed commands. Although the spin period fluctuations were significantly reduced by the torquing maneuver, it returned after a period of time to full pre-torquing magnitude. Another puzzling aspect of the spin rate ripple was the period. Instead of the expected antisymmetric mode period of 12.8 seconds associated with two radial 14.5 meter tape ribbon booms, a period of 13.2 seconds was observed. The symmetric mode vibration period, which was not observable with the on-board sun sensor, had a period of 13.5 seconds. Longman and Massart in Reference 1 give a resume of events that took place. After examining possible perturbing effects, they felt that solar pressure acting on the two radial 14.5 meter tape booms having small tip masses might be the cause of the spin rate ripple. Subsequent theoretical analysis and computer simulations did not sustain the solar pressure effect hypothesis. It is the intent of this paper to show that thermal contraction and expansion of the 14.5 meter ribbon booms going in and out of the spacecraft hub shadow could be a reasonable explanation of the observed spin rate ripple phenomenon. The sun's rays were essentially perpendicular to the spin axis of the spacecraft, at times perpendicular to the wide surface of the ribbon during a rotation period and hub shadowing of the ribbons does take place. The equations of motion and related thermal equations for this situation will now be developed.

ORIGINAL PAGE IS
OF POOR QUALITY

2. EQUATIONS OF MOTION

As stated in Reference 1, the observed sun sensor data from ISEE-B indicated that there was no steady state nutation motion, that the dynamic motion of the spacecraft and flexible booms was essentially planar. This greatly simplifies the mathematical formulation and analysis of the problem. Figure 1 shows a sketch of the spacecraft with appendages.

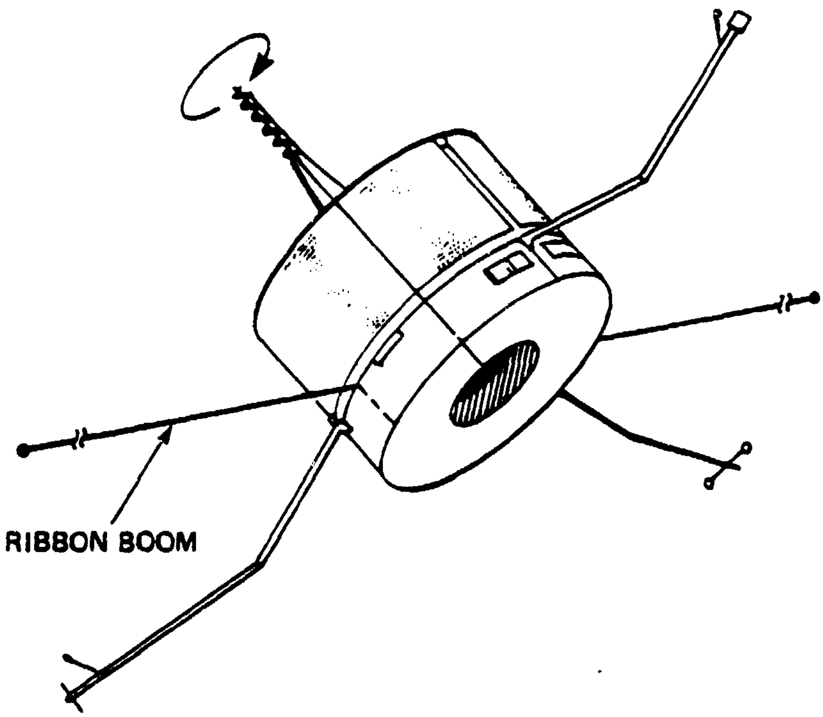

Figure 1. ISEE-B Spacecraft

The main focus of attention is the rigid hub and the two 14.5 meter ribbon booms. The ribbon booms are made of beryllium copper with a width of 0.5 centimeter (0.197 inch) and a thickness of 0.04 centimeter (0.0157 inch). Figure 2 defines the planar coordinate systems used in this analysis.

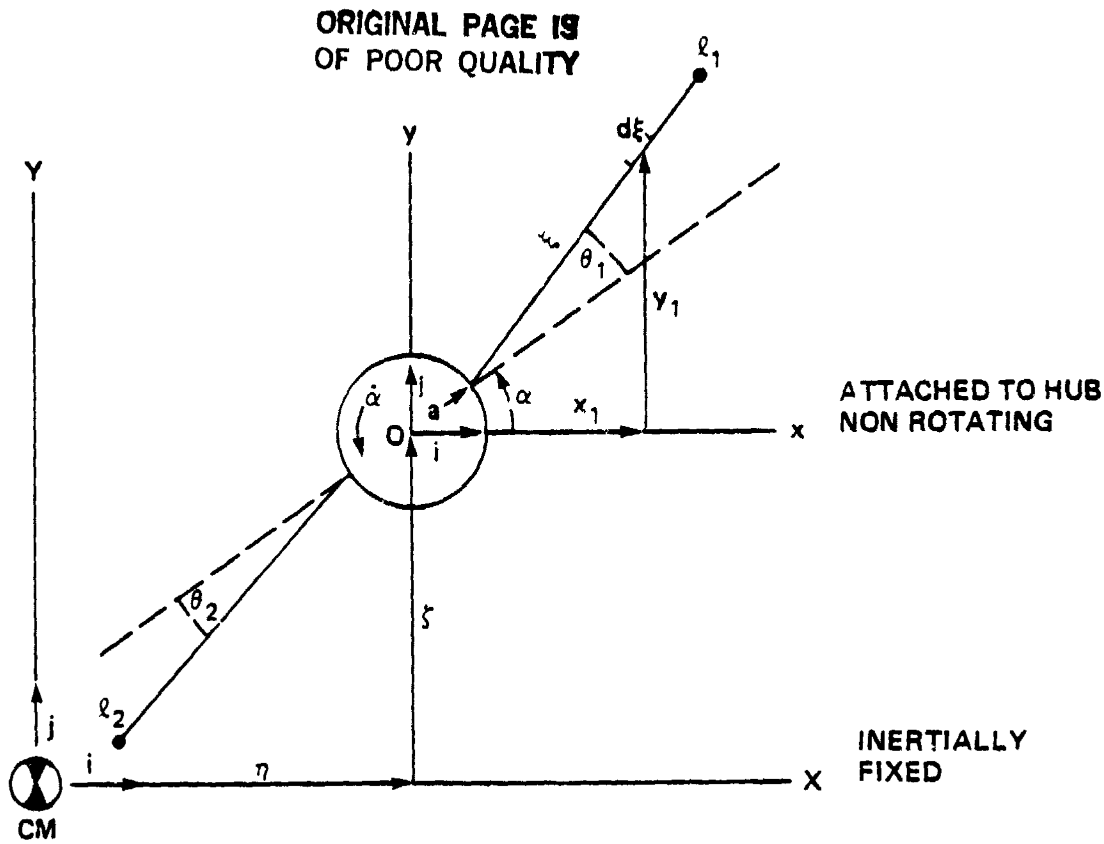

Figure 2. Coordinate System

Since a force-free system is being considered, the origin of the reference coordinate system is located at the center of mass of the hub-booms system. The usual assumption of attitude motion uncoupled from the spacecraft orbit is made and so the center of mass is considered fixed (or moving with constant velocity). The spacecraft hub is allowed two linear degrees of freedom in a plane plus rotation. The ribbons and tip masses are modelled as physical pendula hinged at their base. This latter consideration models the lowest vibration modes of the ribbon with reasonable accuracy.

The Lagrangian method will be used to obtain the equations of motion. This requires determining, in this case, only the total kinetic energy of the system. Let $\vec{R}$ be a vector from the center of mass of the system to any point on the spacecraft and $\dot{\vec{R}}$ the total time derivative of the position vector, then the total kinetic energy of the system and also the Lagrangian is

ORIGINAL PAGE IS
OF POOR QUALITY

$$T = \frac{1}{2}\int_{S/C} \dot{\vec{R}} \cdot \dot{\vec{R}}\, dm \tag{1}$$

where dm is an increment of mass and the integration is over the entire spacecraft. To simplify the analysis, in the derivation of the kinetic energy of the spacecraft, the contribution of $\dot{\ell}$ to the total kinetic energy will be neglected, but $\dot{\ell}$ in the equations of motion will be retained. It will be seen that this is adequate to reveal the phenomenon under consideration. Let $\vec{R}_0$ be a vector from the center of mass to the center of the hub and $\vec{r}$ a vector from the hub center to a point on the spacecraft. Then the following can be written

$$\vec{R} = \vec{R}_0 + \vec{r}$$

$$\vec{R}_0 = \eta i + \zeta j,\ \dot{\vec{R}}_0 = \dot{\eta} i + \dot{\zeta} j$$

$$\vec{r} = xi + yj,\ \dot{\vec{r}} = \dot{x}i + \dot{y}j$$

hence

$$\dot{\vec{R}} = (\dot{\eta} + \dot{x})i + (\dot{\zeta} + \dot{y})j \tag{2}$$

where i and j are unit vectors as shown in Figure 2. In taking the time derivatives, there is no $\vec{\omega}$ cross terms because the coordinate systems are not rotating. Substituting Equation 2 into Equation 1 and carrying out the vector dot product results in

$$T = \frac{1}{2}\int_{S/C} (\dot{\eta}^2 + \dot{\zeta}^2)dm + \frac{1}{2}\int_{S/C} (\dot{x}^2 + \dot{y}^2)dm + \int_{S/C} (\dot{\eta}\dot{x} + \dot{\zeta}\dot{y})dm \tag{3}$$

It will be noticed in Equation 3 that the first integral relates to translation, the second integral relates to rotation and the third integral relates to translation-rotation coupling.

Since $\dot{\eta}$ and $\dot{\zeta}$ are independent of the spacecraft mass distribution, the first integral can be integrated to give

$$\int_{S/C} (\dot{\eta}^2 + \dot{\zeta}^2)dm = M_T(\dot{\eta}^2 + \dot{\zeta}^2) \tag{4}$$

where M_T is the total mass of the spacecraft.

ORIGINAL PAGE IS
OF POOR QUALITY

In general, the dynamic system that we are considering has the degrees of freedom: η, ζ, α, x and y or as will be seen subsequently, η, ζ, α, θ_1 and θ_2. The third integral in Equation 3 can be evaluated in the following way: the equation of motion for the η direction using the Lagrangian method is

$$\frac{d}{dt}\left(\frac{\partial T}{\partial \dot{\eta}}\right) - \frac{\partial T}{\partial \eta} = Q_\eta = 0 \tag{5}$$

Now from Equation 3, $\frac{\partial T}{\partial \eta} = 0$, hence Equation 5 can be integrated to

$$\frac{\partial T}{\partial \dot{\eta}} = \text{constant} \tag{6}$$

Evaluating $\frac{\partial T}{\partial \dot{\eta}}$ from Equation 3 and 4 gives

$$\frac{\partial T}{\partial \dot{\eta}} = M_T\dot{\eta} + \int_{S/C} \dot{x}\, dm = \text{constant} \tag{7}$$

At t = 0, everything is assumed quiescent: $\dot{\eta} = \dot{x} = 0$, hence the constant in Equation 7 is found to be zero and

$$\dot{\eta}M_T = -\int_{S/C} \dot{x}\, dm \tag{8}$$

In a similar manner for the ζ linear direction results in

$$\dot{\zeta}M_T = -\int_{S/C} \dot{y}\, dm \tag{9}$$

Using Equations 8 and 9 and noting that $\dot{\eta}$ and $\dot{\zeta}$ do not depend on the integration over the S/C, the third integral in Equation 3 evaluates to

$$\int_{S/C} (\dot{\eta}\dot{x} + \dot{\zeta}\dot{y})dm = -M_T(\dot{\eta}^2 + \dot{\zeta}^2) \tag{10}$$

The Lagrangian thus far can be written as

$$T = \frac{1}{2}\int_{S/C} (\dot{x}^2 + \dot{y}^2)dm - \frac{1}{2}M_T(\dot{\eta}^2 + \dot{\zeta}^2) \tag{11}$$

ORIGINAL PAGE IS
OF POOR QUALITY

Continuing further to eventually express η and ζ in terms of angular displacements of the ribbon so that the Lagrangian can be completely expressed in terms of these angular displacements, Equations 8 and 9 can be integrated once more to give

$$\eta M_T = -\int_{S/C} x \, dm \tag{12a}$$

and

$$\zeta M_T = -\int_{S/C} y \, dm \tag{12b}$$

Note that Equations 12a, b are simply the first mass moment equations. Using the transformation

$$\begin{aligned} x_1 &= a \cos \alpha + \xi \cos (\theta_1 + \alpha), \; x_2 = a \cos (\alpha + \pi) + \xi \cos (\theta_2 + \alpha + \pi) \\ y_1 &= a \sin \alpha + \xi \sin (\theta_1 + \alpha), \; y_2 = a \sin (\alpha + \pi) + \xi \sin (\theta_2 + \alpha + \pi) \end{aligned} \tag{13}$$

where a is the radius of the hub, ξ is the distance along the wire to the increment of mass and carrying out the integration indicated by Equations 12a and 12b (the hub does not contribute):

$$\eta M_T = -\int_{\substack{\text{wire \&} \\ \text{tip mass}}} \rho x_1 \, d\xi - \int_{\substack{\text{wire \&} \\ \text{tip mass}}} \rho x_2 \, d\xi \tag{13a}$$

$$\zeta M_T = -\int_{\substack{\text{wire \&} \\ \text{tip mass}}} \rho y_1 \, d\xi - \int_{\substack{\text{wire \&} \\ \text{tip mass}}} \rho y_2 \, d\xi \tag{13b}$$

where ρ is the nominal mass per unit length of the wire, results in

$$\eta M_T = -(\rho \ell^2/2 + m\ell)[\cos (\theta_1 + \alpha) - \cos (\theta_2 + \alpha)] \tag{14a}$$

$$\zeta M_T = -(\rho \ell^2/2 + m\ell)[\sin (\theta_1 + \alpha) - \sin (\theta_2 + \alpha)] \tag{14b}$$

where an average wire length, ℓ, has been used to simplify the algebra for this part of the kinetic energy and m is the tip mass.

ORIGINAL PAGE IS
OF POOR QUALITY

Differentiating Equations 14a and 14b and dividing by M_T gives the spacecraft translation velocities in terms of the angular motion of the hub and ribbons

$$\dot{\eta} = \frac{(\rho \ell^2/2 + m\ell)}{M_T} [(\dot{\theta}_1 + \dot{\alpha}) \sin (\theta_1 + \alpha) - (\dot{\theta}_2 + \dot{\alpha}) \sin (\theta_2 + \alpha)] \tag{15a}$$

$$\dot{\zeta} = - \frac{(\rho \ell^2/2 + m\ell)}{M_T} [(\dot{\theta}_1 + \dot{\alpha}) \cos (\theta_1 + \alpha) - (\dot{\theta}_2 + \dot{\alpha}) \cos (\theta_2 + \alpha)] \tag{15b}$$

Squaring Equations 15a and 15b, adding and multiplying by M_T gives

$$M_T (\dot{\eta}^2 + \dot{\zeta}^2) = M_c [(\dot{\theta}_1 + \dot{\alpha})^2 + (\dot{\theta}_2 + \dot{\alpha})^2 - 2(\dot{\theta}_1 + \dot{\alpha})(\dot{\theta}_2 + \dot{\alpha})] \cos (\theta_1 - \theta_2) \tag{16}$$

where M_c is defined as

$$M_c = \frac{(\rho \ell^2/2 + m\ell)^2}{M_T} \tag{17}$$

and ℓ is an average length, $\frac{\ell_1 + \ell_2}{2}$,

In a somewhat similar manner, the integral in Equation 11 related to the rotational kinetic energy, T_R, can be evaluated

$$\begin{aligned} T_R = & \frac{1}{2} I \dot{\alpha}^2 + \frac{1}{2} [(\rho \ell_1 + m_1) a^2 \dot{\alpha}^2 + 2(\rho \ell_1^2/2 + m_1) a \dot{\alpha} (\dot{\theta}_1 + \dot{\alpha}) \cos \theta_1 \\ & + (m_1 \ell_1^2 + \rho \ell_1^3/3)(\dot{\theta}_1 + \dot{\alpha})^2] \\ & + \frac{1}{2} [(\rho \ell_2 + m_2) a^2 \dot{\alpha}^2 + 2 (\rho \ell_2^2/2 + m\ell_2) a \dot{\alpha} (\dot{\theta}_2 + \dot{\alpha}) \cos \theta_2 \\ & + (m_2 \ell_2^2 + \rho \ell_2^2/3)(\dot{\theta}_2 + \dot{\alpha})^2] \end{aligned} \tag{18}$$

In Equation 18, I is the hub moment of inertia and an attempt has been made to include assymmetries caused by different ribbon lengths and tip masses. Initially it was thought that the small difference in tip mass weight might be a contributing factor to the anomaly. This is briefly discussed in Section 5.

Defining the following quantities

ORIGINAL PAGE IS
OF POOR QUALITY

$$M_{11} = a^2(\rho \ell_1 + m_1) \qquad M_{21} = a^2(\rho \ell_2 + m_2)$$

$$M_{12} = a(\rho \ell_1^2/2 + m_1 \ell_1) \qquad M_{22} = a(\rho \ell_2^2/2 + m_2 \ell_2)$$

$$M_{13} = \rho \ell_1^3/3 + m_1 \ell_1^2 \qquad M_{23} = \rho \ell_2^3/3 + m_2 \ell_2^2 \tag{19}$$

and using Equations 11, 16, 18 and 19, the Lagrangian (total kinetic energy) can be written as

$$\begin{aligned} T = & \frac{1}{2} I\dot{\alpha}^2 + \frac{1}{2}[M_{11}\dot{\alpha}^2 + 2M_{12}\dot{\alpha}(\dot{\theta}_1 + \dot{\alpha}) \cos \theta_1 + M_{13}(\dot{\theta}_1 + \dot{\alpha})^2] \\ & + \frac{1}{2}[M_{21}\dot{\alpha}^2 + 2M_{22}\dot{\alpha}(\dot{\theta}_2 + \dot{\alpha}) \cos \theta_2 + M_{23}(\dot{\theta}_1 + \dot{\alpha})^2] \\ & - \frac{1}{2}M_c[(\dot{\theta}_1 + \dot{\alpha})^2 + (\dot{\theta}_2 + \dot{\alpha})^2 - 2(\dot{\theta}_1 + \dot{\alpha})(\dot{\theta}_2 + \dot{\alpha}) \cos (\theta_1 - \theta_2)] \end{aligned} \tag{20}$$

The remaining angular equations of motion can now be written. For θ_1,

$$\frac{d}{dt}\left(\frac{\partial T}{\partial \dot{\theta}_1}\right) - \frac{\partial T}{\partial \theta_1} = Q_{\theta_1} = -c\dot{\theta}_1 \tag{21a}$$

or in integral form

$$\frac{\partial T}{\partial \dot{\theta}_1} = \left.\frac{\partial T}{\partial \dot{\theta}_1}\right]_{t=0} + \int_0^t \left(\frac{\partial T}{\partial \theta_1} - c\dot{\theta}_1\right) dt \tag{21b}$$

where

$$\frac{\partial T}{\partial \dot{\theta}_1} = M_{12}\dot{\alpha} \cos \theta_1 + M_{13}(\dot{\theta}_1 + \dot{\alpha}) - M_c[\dot{\theta}_1 + \dot{\alpha} - (\dot{\theta}_2 + \dot{\alpha}) \cos (\theta_1 - \theta_2)] \tag{22}$$

$$\frac{\partial T}{\partial \theta_1} = -M_{12}(\dot{\theta}_1 + \dot{\alpha}) \sin \theta_1 - M_c(\dot{\theta}_1 + \dot{\alpha})(\dot{\theta}_2 + \dot{\alpha}) \sin (\theta_1 - \theta_2) \tag{23}$$

and $-c\dot{\theta}_1$ is a damping term due to combined ribbon and spacecraft damping. For θ_2,

$$\frac{d}{dt}\left(\frac{\partial T}{\partial \dot{\theta}_2}\right) - \frac{\partial T}{\partial \theta_2} = Q_{\theta_2} = -c\dot{\theta}_2 \tag{24a}$$

or in integral form

$$\frac{\partial T}{\partial \dot{\theta}_2} = \left.\frac{\partial T}{\partial \dot{\theta}_2}\right]_{t=0} + \int_0^t \left(\frac{\partial T}{\partial \theta_1} - c\dot{\theta}_2\right) dt \tag{24b}$$

ORIGINAL PAGE IS
OF POOR QUALITY

where

$$\frac{\partial T}{\partial \dot{\theta}_2} = M_{22}\dot{\alpha}\cos\theta_2 + M_{23}(\dot{\theta}_2 + \dot{\alpha}) - M_c[\dot{\theta}_2 + \dot{\alpha} - (\dot{\theta}_1 + \dot{\alpha})\cos(\theta_1 - \theta_2)] \tag{25}$$

$$\frac{\partial T}{\partial \theta_2} = -M_{2}\text{[illegible]}_2 + \dot{\alpha})\sin\theta_2 + M_c(\dot{\theta}_1 + \dot{\alpha})(\dot{\theta}_2 + \dot{\alpha})\sin(\theta_1 - \theta_2) \tag{26}$$

and $-c\dot{\theta}_2$ is a boom motion damping term.

For α,

$$\frac{d}{dt}\left(\frac{\partial T}{\partial \dot{\alpha}}\right) - \frac{\partial T}{\partial \alpha} = Q_\alpha = 0 \tag{27}$$

where

$$\begin{aligned}\frac{\partial T}{\partial \dot{\alpha}} = {} & I\dot{\alpha} + M_{11}\dot{\alpha} + M_{11}(\dot{\theta}_1 + 2\dot{\alpha})\cos\theta_1 + M_{12}(\dot{\theta}_1 + \dot{\alpha}) \\ & + M_{21}\dot{\alpha} + M_{22}(\dot{\theta}_2 + 2\dot{\alpha})\cos\theta_2 + M_{23}(\dot{\theta}_2 + \dot{\alpha}) \\ & - M_c[(\dot{\theta}_1 + \dot{\alpha}) + (\dot{\theta}_2 + \dot{\alpha}) - (\dot{\theta}_1 + \dot{\theta}_2 + 2\dot{\alpha})\cos(\theta_1 - \theta_2)]\end{aligned} \tag{28}$$

and

$$\frac{\partial T}{\partial \alpha} = 0 \tag{29}$$

Now Equation 27 can be integrated directly because of Equation 29; this results in

$$\begin{aligned}& I\dot{\alpha} + M_{11}\dot{\alpha} + M_{11}(\dot{\theta}_1 + 2\dot{\alpha})\cos\theta_1 + M_{13}(\dot{\theta}_1 + \dot{\alpha}) \\ & + M_{21}\dot{\alpha} + M_{22}(\dot{\theta}_2 + 2\dot{\alpha})\cos\theta_2 + M_{23}(\dot{\theta}_2 + \dot{\alpha}) \\ & - M_c[(\dot{\theta}_1 + \dot{\alpha}) + (\dot{\theta}_2 + \dot{\alpha}) - (\dot{\theta}_1 + \dot{\theta}_2 + 2\dot{\alpha})\cos(\theta_1 - \theta_2)] = \text{constant} = H_0\end{aligned} \tag{30}$$

which is the conservation of angular momentum equation, since no external torques are considered acting.

3. LINEARIZED EQUATIONS OF MOTION

The partially linearized equations of motion (derived from Equation 21b and 24b) taking into account time variations of ribbon length can be written as

$$M_{13}(\ddot{\theta}_1 + \ddot{\alpha}) + M_{12}\ddot{\alpha} + (\dot{M}_{13} + \dot{M}_{12})\dot{\alpha} - M_c(\ddot{\theta}_1 - \ddot{\theta}_2) - \dot{M}_c(\dot{\theta}_1 - \dot{\theta}_2)$$
$$+ c\dot{\theta}_1 + M_{12}\dot{\alpha}^2\theta_1 + M_c\dot{\alpha}^2(\theta_1 - \theta_2) = 0 \tag{31}$$

and

$$M_{23}(\ddot{\theta}_2 + \ddot{\alpha}) + M_{22}\ddot{\alpha} + (\dot{M}_{23} + \dot{M}_{22})\dot{\alpha} + M_c(\ddot{\theta}_1 - \ddot{\theta}_2) + \dot{M}_c(\dot{\theta}_1 - \dot{\theta}_2)$$
$$+ c\dot{\theta}_2 + M_{22}\dot{\alpha}^2\theta_2 - M_c\dot{\alpha}^2(\theta_1 - \theta_2) = 0 \tag{32}$$

From the definition of the M's, we note that

$$\dot{M}_{13} + \dot{M}_{12} = \frac{1}{a}(2M_{12} + M_{11})\dot{\ell}_1 \tag{33a}$$

$$\dot{M}_{23} + \dot{M}_{22} = \frac{1}{a}(2M_{22} + M_{21})\dot{\ell}_2. \tag{33b}$$

It is convenient to express the linearized equations of motion in terms of normal modes of vibration: antisymmetric mode, $\phi_1 = \theta_1 + \theta_2$, and symmetric mode, $\phi_2 = \theta_1 - \theta_2$. Adding Equations 31 and 32 and considering

$$M_{23} \approx M_{13}, M_{22} \approx M_{12},$$

both constant and from the linearized conservation of angular momentum (Equation 30)

$$\dot{\alpha} \approx \omega_o - \frac{I_w}{I_s}\dot{\phi}_1, \ddot{\alpha} \approx -\frac{I_w}{I_s}\ddot{\phi}_1 \tag{34}$$

we can express the ϕ_1 mode differential equation as

$$I_N\ddot{\phi}_1 + c\dot{\phi}_1 + M_{12}\omega_o{}^2\phi_1 = -\frac{1}{a}(2M_{12} + M_{11})(\dot{\ell}_1 + \dot{\ell}_2)\omega_o \tag{35}$$

where

$$I_N = M_{13} - 2\frac{I_w}{I_s}(M_{13} + M_{12})$$

and ω_o is the nominal spin rate. For the ϕ_2 mode differential equation we can write

$$(M_{13} - 2M_c)\ddot{\phi}_2 + c\dot{\phi}_2 + (M_{12} + 2M_c)\,\omega_o^2\phi_2 = -\frac{1}{a}(2M_{12} + M_{11})(\dot{\ell}_1 - \dot{\ell}_2)\omega_o \qquad (36)$$

Both equations are considered to have constant coefficients. From the right hand side of Equations 35 and 36 we see the potentially driving nature of time varying ribbon lengths that can come from contraction and expansion of the ribbon booms going into and out of the spacecraft hub shadow.

4. THERMAL EFFECTS

Additional equations are required for the contraction and expansion of the ribbon going in and out of the shadow of the spacecraft hub. Initially the ribbon will be divided up into small typical elements and shadowing effects brought in by averaging over a spin period; subsequently the elements are sumed for the total thermal displacement. The thermal effect will be modeled as a first order lag differential equation of the form

$$\dot{\delta}_j + \frac{1}{\tau}\delta_j = \frac{\delta_{s_j}}{\tau}F_j(\beta) \qquad (37)$$

where δ_j is the thermal change in length of a small ribbon element, τ is the characteristic time constant of the thermal effect, δ_{s_j} is the steady state value and F_j is a shadowing factor: 1 in the sunlight and 0 in complete shadow; β is the angular location of the small element about the spin axis (see Figure 3). For simplicity, conduction along the ribbon is neglected. Equation 37 is related to a linearization of a heat balance between heat storage loss and radiation to space plus the relationship between thermal displacement and temperature difference.

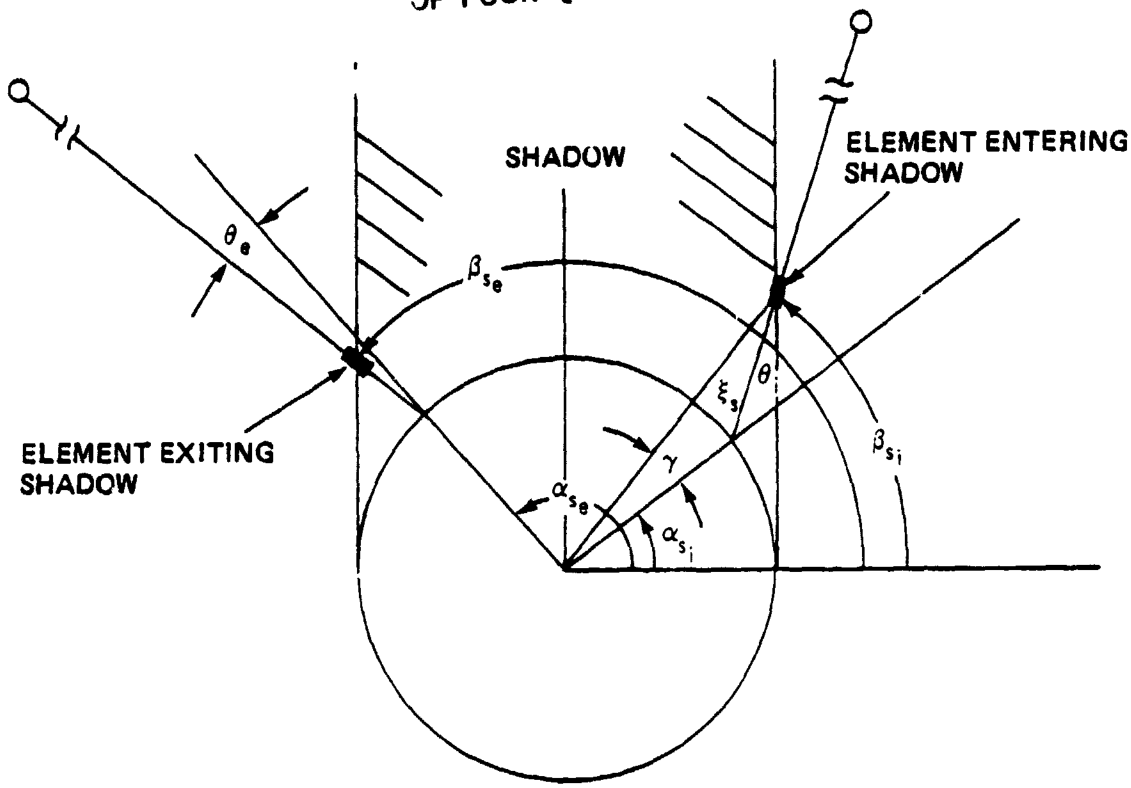

Figure 3. Entering and Exiting Shadow Geometry

We are mainly interested in long term effects. Equation 37 will be averaged over a hub rotation to take out the time consuming spin rate dependence. This procedure essentially retains the symmetric and antisymmetric frequencies (which are lower than the spin rate by a factor greater than four) and effectively results in using only the "constant" term in a Fourier series expansion of $F_j(\beta)$. Averaging Equation 37 results in

$$\dot{\delta}_j + \frac{1}{\tau}\delta_j = \frac{\delta_{s_j}}{\tau 2\pi}\oint F_j(\beta)d\alpha \qquad (38)$$

Referring to Figure 3 the integral on the right hand side of Equation 38 can be written as

$$\frac{1}{2\pi}\oint F_j(\beta)d\alpha = \frac{1}{2\pi}\Bigg\{\int_0^{\alpha_{s_i}} 1d\alpha + \int_{\alpha_{s_i}}^{\alpha_{s_e}} 0d\alpha + \int_{\alpha_{s_e}}^{2\pi} 1d\alpha = \frac{1}{2\pi}\Big\{\alpha_{s_i} - \alpha_{s_e} + 2\pi\Big\} \qquad (39)$$

where α_{s_i} is the hub rotation angle going into the shadow of the j^{th} element and α_{s_e} is the exiting angle from the shadow. Now the onset of shadowing for each element is given by the following condition, linearized for small ribbon angles

$$(a + \xi_s) \cos \beta_{s_i} = a$$

or

$$\beta_{s_i} = \arccos \frac{a}{a + \xi_s} \tag{40}$$

where ξ_s identifies the element going into the shadow. The linearized condition for exiting the shadow is given by

$$(a + \xi_s) \cos \beta_{s_e} = -a$$

or

$$\beta_{s_e} = \arccos \left(- \frac{a}{a + \xi_s} \right) \tag{41}$$

For small ribbon angles, the following geometric relations can be written from Figure 3

$$\beta_{s_i} = \alpha_{s_i} + \gamma_i \approx \alpha_{s_i} + \frac{\xi_s \theta_i}{a + \xi_s}$$

or

$$\alpha_{s_i} = \beta_{s_i} - \frac{\xi_s \theta_i}{a + \xi_s} \tag{42}$$

and

$$\beta_{s_e} = \alpha_{s_e} + \gamma_e \approx a_{s_i} + \frac{\xi_s \theta_e}{a + \xi_s}$$

or

$$\alpha_{s_e} = \beta_{s_e} - \frac{\xi_s \theta_e}{a + \xi_s} \tag{43}$$

ORIGINAL PAGE IS
OF POOR QUALITY

Using Equations 40, 41, 42 and 43 and forming the difference $\alpha_i - \alpha_e$, we arrive at

$$\alpha_{s_i} - \alpha_{s_e} = \arccos\left(\frac{a}{a+\xi_s}\right) - \arccos\left(-\frac{a}{a+\xi_s}\right) + \frac{\xi_s}{a+\xi_s}(\theta_e - \theta_i) \tag{44}$$

Since

$$\arccos(x) + \arccos(-x) = \pi \tag{45}$$

the above equation can be written

$$\alpha_{s_i} - \alpha_{s_e} = 2\arccos\left(\frac{a}{a+\xi_s}\right) + \frac{\xi_s}{a+\xi_s}(\theta_e - \theta_i) - \pi \tag{46}$$

Now strictly speaking, θ_i and θ_e vary somewhat as one goes along the ribbon length entering and exiting the shadow. Neglecting this effect and defining $\theta_e - \theta_i = -\theta$ as the net angular motion generated going through the hub shadow, Equation 38 (using Equations 39 and 46) for ribbon 1 becomes

$$\dot{\delta}_{1j} + \frac{1}{\tau}\delta_{1j} = \frac{\delta_{s_j}}{2\pi\tau}\left\{\pi + 2\arccos\left(\frac{a}{a+\xi_s}\right) - \frac{\xi_s\theta_1}{a+\xi_s}\right\} \tag{47}$$

For ribbon 2 we have

$$\delta_{2j} + \frac{1}{\tau}\delta_{2j} = \frac{\delta_{s_j}}{2\pi\tau}\left\{\pi + 2\arccos\left(\frac{a}{a+\xi_s}\right) - \frac{\xi_s\theta_2}{a+\xi_s}\right\} \tag{48}$$

Basically the right hand side of Equations 47 and 48 (braces divided by 2π) is a measure of the fraction of a rotation period that is spent in the sunlight by an element. The minus sign is chosen for the net angular motion (and also guided by the subsequent results) because as the ribbon enters the shadow, Coriolis forces (caused by contraction) urge the ribbon forward into the shadow; as the ribbon comes out of the shadow, Coriolis forces (now caused by expansion) tend to keep the ribbon in the shadow; this effectively reduces the time in the sunlight and the negative sign reflects this. Thus we see that the ribbon angular motion can affect the thermally induced displacements by the time spent in the sunlight/shadow. This is a possible mechanism for solar thermal energy to be delivered to the dynamic system.

Summing over all of the small elements to obtain the total ribbon thermal displacements gives

$$\sum_j \delta_{1j} = \delta_1 \tag{49a}$$

$$\sum_j \delta_{2j} = \delta_2 \tag{49b}$$

Note that $\ell_1 = \ell_0 + \delta_1$ and $\ell_2 = \ell_0 + \delta_2$ where ℓ_0 is the nominal length of the ribbon. Equations 47 and 48 become

$$\dot{\delta}_1 + \frac{1}{\tau}\delta_1 = \frac{1}{2\pi\tau}\sum_j \delta_{sj}\left\{\pi + 2\,\text{arcos}\left(\frac{a}{a+\xi_s}\right) - \frac{\xi_s\theta_1}{a+\xi_s}\right\} \tag{50a}$$

$$\dot{\delta}_2 + \frac{1}{\tau}\delta_2 = \frac{1}{2\pi\tau}\sum_j \delta_{sj}\left\{\pi + 2\,\text{arcos}\left(\frac{a}{a+\xi_s}\right) - \frac{\xi_s\theta_2}{a+\xi_s}\right\}. \tag{50b}$$

Now the right hand side of Equations 50a and b can be converted to integrals by noting that

$$\delta_{s_j} \approx \delta_s\left(\frac{\Delta\xi}{\ell}\right) \tag{51}$$

Each infinitesimal element contributes a fraction, $\frac{\Delta\xi}{\ell}$, to the total steady state change of length, δ_s. We thus have

$$\dot{\delta}_1 + \frac{1}{\tau}\delta_1 = \frac{\delta_s}{2\pi\tau}\left\{\pi + \frac{2}{\ell}\int_0^{\ell} \text{arcos}\left(\frac{a}{a+\xi}\right)\,d\xi - \frac{1}{\ell}\int_0^{\ell}\frac{\xi_s\theta_1}{a+\xi_s}\,d\xi\right\} \tag{52a}$$

and

$$\dot{\delta}_2 + \frac{1}{\tau}\delta_2 = \frac{\delta_s}{2\pi\tau}\left\{\pi + \frac{2}{\ell}\int \text{arcos}\left(\frac{a}{a+\xi}\right)\,d\xi - \frac{1}{\ell}\int_0^{\ell}\frac{\xi_s\theta_2}{a+\xi_s}\,d\xi\right\} \tag{52b}$$

where

$$\sum_j \delta_{s_j} = \delta_s \tag{53}$$

the total steady state change of length of the ribbon, and integration is indicated for the second and third terms. Carrying out the integrations and defining quantities results in the compact form

$$\dot{\delta}_1 + \frac{1}{\tau}\delta_1 = \frac{\delta_s}{\tau}(e - k\theta_1) \tag{54a}$$

$$\dot{\delta}_2 + \frac{1}{\tau}\delta_2 = \frac{\delta_s}{\tau}(e - k\theta_2) \tag{54b}$$

where

$$e = \frac{1}{2\pi}\left\{\pi + 2(1 + a/\ell)\arccos\frac{a}{a+\ell} - \frac{2a}{\ell}\ln\frac{(a + \ell + \sqrt{\ell^2 + 2a\ell})}{a}\right\} \tag{55}$$

and

$$k = \frac{1}{2\pi}\left\{1 - \frac{a}{\ell}\ln(1 + \ell/a)\right\} \tag{56}$$

The length ℓ considered here is the nominal length of the ribbon. Using operator notation ($d/dt \equiv D$), Equations 54a, b can be written as

$$\left(D + \frac{1}{\tau}\right)\delta_1 = \frac{\delta_s}{\tau}(e - k\theta_1) \tag{57a}$$

$$\left(D + \frac{1}{\tau}\right)\delta_2 = \frac{\delta_s}{\tau}(e - k\theta_2) \tag{57b}$$

and the component of the averaged steady state solution depending on the ribbon angles can be expressed symbolically as

$$\delta_1 = -\frac{\delta_s k\theta_1}{(\tau D + 1)} \tag{58a}$$

$$\delta_2 = -\frac{\delta_s k\theta_2}{(\tau D + 1)} \tag{58b}$$

We can thus write the sum and difference of the thermal effect of the ribbons in terms of the ϕ_1, ϕ_2 modes

$$\dot{\delta}_1 + \dot{\delta}_2 = \dot{\ell}_1 + \dot{\ell}_2 = -\frac{\delta_s k\dot{\phi}_1}{\tau D + 1} \tag{59a}$$

ORIGINAL PAGE IS
OF POOR QUALITY

and

$$\dot{\delta}_1 - \dot{\delta}_2 = \dot{\ell}_1 - \dot{\ell}_2 = -\frac{\delta_s k \dot{\phi}_2}{\tau D + 1} \tag{59b}$$

5. ANALYSIS AND INTERPRETATION OF RESULTS

We are now in a position to return to the linearized equations of motion and evaluate the effect of the thermally induced ribbon displacements. Substituting Equation 59a into Equation 35 and Equation 59b into Equation 36 results in the governing dynamic-thermal differential equations for the ϕ_1 and ϕ_2 modes

$$I_N \ddot{\phi}_1 + \left[c - \frac{\delta_s k \omega_o}{a} \frac{(2M_{12} + M_{11})}{(\tau D + 1)} \right] \dot{\phi}_1 + M_{12} \omega_o^2 \phi_1 = 0 \tag{60a}$$

and

$$(M_{13} - 2M_c) \ddot{\phi}_2 + \left[c - \frac{\delta_s k \omega_o}{a} \frac{(2M_{12} + M_{11})}{(\tau D + 1)} \right] \dot{\phi}_2 + (M_{12} + 2M_c) \omega_o^2 \phi_2 = 0 \tag{60b}$$

Focusing on the antisymmetric mode, ϕ_1, the nature of the motion can be ascertained by assuming τ small and expanding the operator

$$\frac{1}{1 + \tau D} \approx 1 - \tau D \ldots . \tag{61}$$

in Equation 60 a. After rearranging one can write

$$\ddot{\phi}_1 - \frac{\left[\frac{\delta_s}{a} k \omega_o (2M_{12} + M_{11}) - c \right]}{I_N + \frac{\tau \omega_o \delta_s k}{a} (2M_{12} + M_{11})} \dot{\phi}_1 + \frac{M_{12} \omega_o^2 \phi_1}{I_N + \frac{\tau \omega_o \delta_s k}{a} (2M_{12} + M_{11})} = 0 \tag{62}$$

Let

$$2\mu\Omega = \frac{\frac{\delta_s}{a} k \omega_o (2M_{12} + M_{11}) - c}{I_N + \frac{\tau \omega_o \delta_s k}{a} (2M_{12} + M_{11})} \tag{63}$$

ORIGINAL PAGE IS
OF POOR QUALITY

and

$$\Omega^2 = \frac{M_{12}\omega_o^2}{I_N + \frac{\tau\omega_o\delta_s k}{a}(2M_{12} + M_{11})} \tag{64}$$

Equation 62 can be put into the standard 2nd order differential equation

$$\ddot{\phi}_1 - 2\mu\Omega\dot{\phi}_1 + \Omega^2\phi_1 = 0 \tag{65}$$

which has the solution

$$\phi_1 = Ae^{\mu\Omega t}\sin\sqrt{1-\mu^2}\,\Omega t + Be^{\mu\Omega t}\cos\sqrt{1-\mu^2}\,\Omega t \tag{66}$$

where A and B are constants. For combined ribbon and spacecraft damping less than the thermal driving term

$$c < \delta_s k\omega_o(2M_{12} + M_{11})/a$$

μ is positive, we note that the amplitude of the antisymmetric mode increases exponentially, also note from Equation 64 that the frequency is reduced by the τ term. A similar result can be obtained for the symmetric ϕ_2 mode.

Figure 4 shows some spin ripple amplitude flight data (taken from reference 1) after a torquing maneuver on April 23, 1980. Immediately after the maneuver, a divergent time constant of approximately 3.6 days was calculated. To show some quantitative results from this analysis, Equation 60a was cleared of the $1 + \tau D$ operator in the denominator of the first derivative tenn and only linear terms were retained. This results in a third order differential equation for ϕ_1,

$$\tau I_N\dddot{\phi}_1 + (I_N + c\tau)\ddot{\phi}_1 + (c + \tau M_{12}\omega_o^2 - G)\dot{\phi}_1 + M_{12}\omega_o^2\phi_1 = 0 \tag{67}$$

where

$$G = \delta_s\omega_o k(2M_{12} + M_{11})/a \tag{68}$$

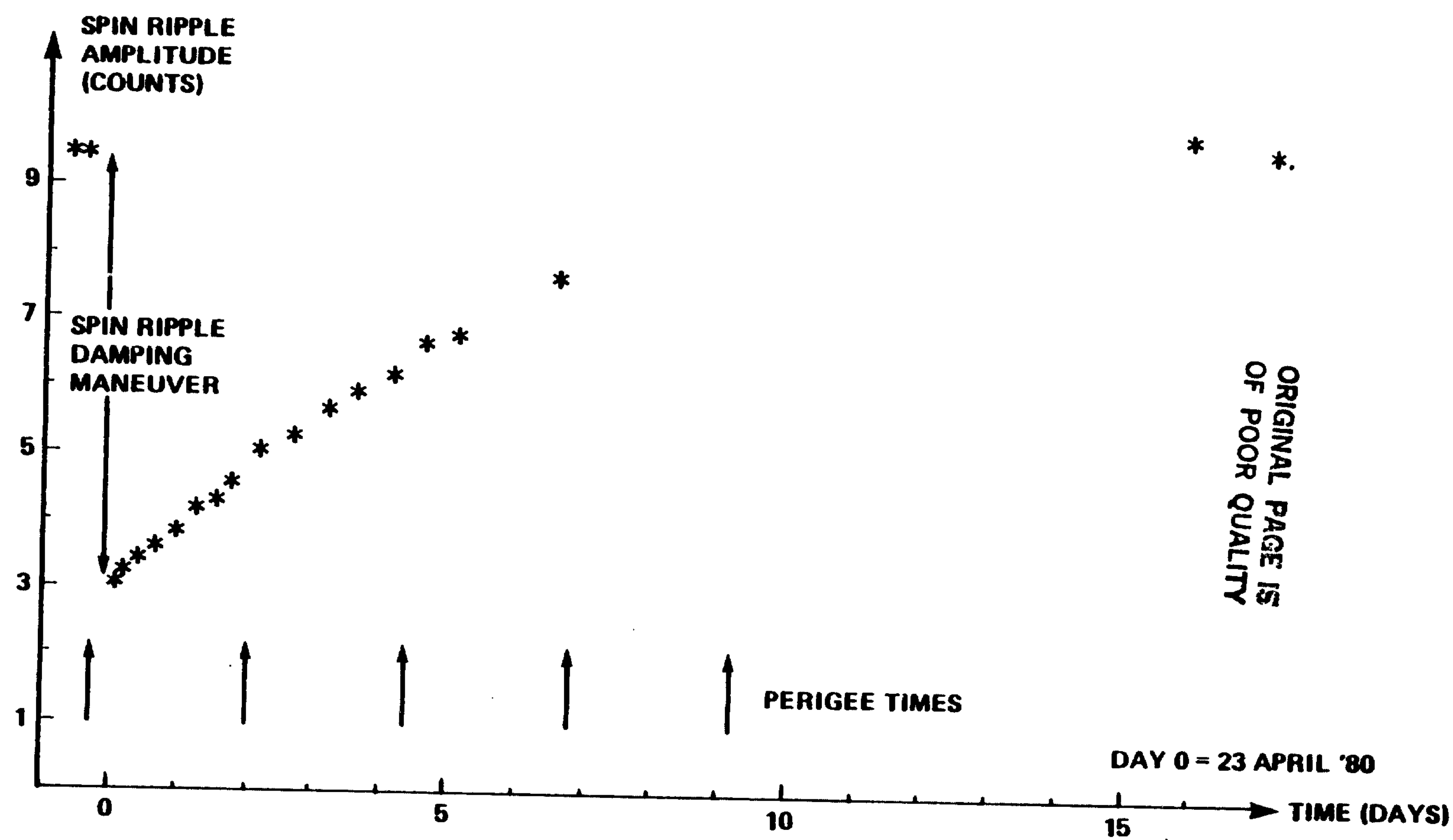

Figure 4. Evolution of Spin Ripple Amplitude Following Ripple Reduction Maneuver (Reference 1)

ORIGINAL PAGE IS
OF POOR QUALITY

For the following spacecraft parameters

$I = 62.033$ slug ft^2 $\rho = 2.8 \times 10^{-5}$ slug/ft

$I_s = 69.79$ slug ft^2 $\delta_s = 0.15$ ft

$a = 2.082$ ft $\omega_0 = 2.0724$ rad/sec

$\ell_0 = 47.54$ ft $k = 0.159$

$c = 0.0$

the roots of the ϕ_1 mode are displayed in Table I as a function of the thermal time constant, τ.

Table I
Roots of Thermally Induced Spin Rate Ripple Equation – Antisymmetric Mode

Tau	Root 1		Root 2		Root 3	
	Real	Imag.	Real	Imag.	Real	Imag.
.0	2.5477E-07	.49120	2.5477E-07	-.19120	-6.6672E-03	.0
5.00000	1.9565E-04	.49074	1.9565E-04	-.49074	-.20039	.0
10.0000	5.5097E-05	.49095	5.5097E-05	-.49095	-.10011	.0
15.0000	2.4842E-05	.49104	2.4842E-05	-.49104	-6.6716E-02	.0
20.0000	1.4097E-05	.49108	1.4097E-05	-.49108	-5.0028E-02	.0
25.0000	9.0796E-06	.49111	9.0796E-06	-.49111	-4.0018E-02	.0
30.0000	6.3078E-06	.49113	6.3078E-06	-.49113	-3.3346E-02	.0
35.0000	4.6525E-06	.49114	4.6525E-06	-.49114	-2.8581E-02	.0
40.0000	3.5606E-06	.49115	3.5606E-06	-.49115	-2.5007E-02	.0
45.0000	2.8137E-06	.49116	2.8137E-06	-.49116	-2.2228E-02	.0
50.0000	2.2806E-06	.49117	2.2806E-06	-.49117	-2.0005E-02	.0
55.0000	1.8836E-06	.49117	1.8836E-06	-.49117	-1.8186E-02	.0
60.0000	1.5833E-06	.49118	1.5833E-06	-.49118	-1.6670E-02	.0
65.0000	1.3459E-06	.49118	1.3459E-06	-.49118	-1.5387E-02	.0
70.0000	1.1642E-06	.49118	1.1642E-06	-.49118	-1.4288E-02	.0
75.0000	1.0129E-06	.49118	1.0129E-06	-.49118	-1.3335E-02	.0
80.0000	8.8824E-07	.49119	8.8824E-07	-.49119	-1.2502E-02	.0
85.0000	7.8724E-07	.49119	7.8724E-07	-.49119	-1.1766E-02	.0
90.0000	7.0257E-07	.49119	7.0257E-07	-.49119	-1.1113E-02	.0
95.0000	6.2844E-07	.49119	6.2844E-07	-.49119	-1.0528E-02	.0
100.000	5.6786E-07	.49119	5.6786E-07	-.49119	-1.0001E-02	.0
105.000	5.1158E-07	.49120	5.1158E-07	-.49120	-9.5248E-03	.0
110.000	4.7019E-07	.49120	4.7019E-07	-.49120	-9.0919E-03	.0
115.000	4.2973E-07	.49120	4.2973E-07	-.49120	-8.6965E-03	.0
120.000	3.9520E-07	.49120	3.9520E-07	-.49120	-8.3341E-03	.0
125.000	3.6588E-07	.49120	3.6588E-07	-.49120	-8.0007E-03	.0
130.000	3.3883E-07	.49120	3.3883E-07	-.49120	-7.6930E-03	.0
135.000	3.1263E-07	.49120	3.1263E-07	-.49120	-7.4080E-03	.0
140.000	2.9051E-07	.49120	2.9051E-07	-.49120	-7.1434E-03	.0
145.000	2.7096E-07	.49120	2.7096E-07	-.49120	-6.8971E-03	.0
150.000	2.5477E-07	.49120	2.5477E-07	-.49120	-6.6672E-03	.0

It will be noted that for a τ of 40 seconds (which does not appear to be unreasonable) a divergent time constant of 3.3 days is possible. In regard to the frequency of oscillation, the frequency is lower (period longer) than without thermal excitation, but it is not as low as what was observed in orbit.

Referring back to Figure 4, it will be noted that the rate of spin ripple amplitude growth decreases with time and eventually stops growing; an essentially "steady state" condition occurs. Now it is inferred that the damping parameter, c, is slowly varying, increasing as the amplitude of ribbon motion increases, eventually limiting the motion. A quasi steady state result can be obtained from this analysis that clearly shows the increase in the antisymmetric mode period. The condition is imposed that the roots of Equation 67 have two purely imaginary roots and one real. This implies a "steady state" sinusoidal motion after the transient damps out. The cubic equation for the roots of Equation 67 should have the form

$$(s + r_1)(s^2 + \Omega^2) = s^3 + r_1 s^2 + \Omega^2 s + r_1 \Omega^2 = 0 \tag{69}$$

The conditions are imposed that

$$r_1 = \frac{1}{\tau} + \frac{c}{I_N}, \qquad \Omega^2 = \frac{c}{\tau I_N} + \frac{\omega_o^2 M_{12}}{I_N} - \frac{G}{\tau I_N}$$

and

$$r_1 \Omega^2 = \frac{M_{12}\omega_o^2}{\tau I_n}$$

Eliminating c from the equations and solving for the frequency results in a quadratic in Ω^2:

$$\tau^2\Omega^4 + (1 + G\tau/I_N - \tau^2\omega_1^2)\Omega^2 - \omega_1^2 = 0 \tag{70}$$

where

$$\omega_1^2 = \frac{M_{12}\omega_o^2}{I_N}$$

the natural frequency of the ϕ_1 antisymmetric mode without the thermal effect. Letting

$$R = \Omega^2/\omega_1^2 \tag{71}$$

Equation 70 can be put into the form

$$\omega_1^2\tau^2R^2 + \left(1 + \frac{G\tau}{I_N} - \tau^2\omega_1^2\right)R - 1 = 0 \tag{72}$$

A simple approximate expression can be obtained for R which reveals the nature of the thermal effect on the natural frequency of the antisymmetric mode by considering

$$R \approx 1 + \epsilon \tag{73}$$

where ϵ is much less than one. Substituting Equation 73 into 72 and neglecting ϵ^2 and solving for ϵ results in

$$\epsilon = -\frac{G\tau/I_N}{1 + G\tau/I_N + \omega_1^2\tau^2} \tag{74}$$

Thus

$$\Omega^2 \approx \omega_1^2\left(1 - \frac{G\tau/I_N}{1 + G\tau/I_N + \omega_1^2\tau^2}\right) \tag{75}$$

We note from Equation 75 that if the thermal time lag is zero or infinite, there is no effect on the "steady state" natural frequency. For any finite value of τ, the natural frequency is less than the frequency without the thermal effect. It can easily be shown that Ω has a minimum when

$$\omega_1\tau = 1 \tag{76}$$

Using this expression in the more accurate Equation 72 results in

$$\Omega^2_{min} \approx \omega_1^2\left(1 - \frac{G}{2\omega_1 I_N}\right) \tag{77}$$

For the previously mentioned spacecraft parameters (except c and δ_s) one can calculate the τ and δ_s required for the observed in-orbit spin rate ripple period. A simple calculation using Equations 72 and 76 to solve for G and hence δ_s gives

$$\tau = 2.04 \text{ seconds}$$

$$\delta_s = 1.71 \text{ ft}$$

It is felt that the necessary time constant is rather short but may be realizable, while the steady state thermal extension is simply too large. The disparity between observed and calculated period could be due to several factors: this analysis has a very simple thermal model to evaluate thermal displacements and shadowing effects (both in a linear sense). A more elaborate thermal model may improve the comparison. Also, nonlinear dynamic coupling of the symmetric and antisymmetric modes could be occurring; or possibly uncertainties in mass properties and linear dimensions could be another. To explore the nonlinear effects due to dynamics and slightly different tip masses, Equations 21b, 24b, 30 and the thermal equations were solved on a digital computer. It was thought that perhaps the unobservable symmetric mode was large due to thermally driven motion and through nonlinear coupling affect the period of oscillation of the smaller amplitude antisymmetric mode. Computer runs showed that for θ_1, θ_2 the order of 0.16, 0.25 radians, respectively, the period of the antisymmetric mode was extended but the oscillations were no longer sinusoidal in form. This approach was dropped.

A practical method to suppress thermally induced spin rate ripple is to utilize an appendage motion damper for the antisymmetric mode (Reference 2). It is a fluid filled ring, tuned to the antisymmetric mode frequency, similar to a passive nutation damper but orientated so that the spin rate fluctuations excite fluid motion. This action dissipates energy through fluid viscous friction and eventually limits the spin rate ripple below discernability. This type of damper was flown on IMP-J, ISEE-A, C and DE-A. All spacecraft had long radial wire appendages subject to thermally induced spin rate ripple. There was no indication of spin rate ripple except going in and coming out of the earth's shadow (ISEE-A and DE-A) which was rapidly eliminated by the damper.

In summary, it is felt that the spin rate ripple anomaly observed on ISEE-B can be explained in terms of a thermally induced hypothesis that couples the ribbon angular motion with the thermally induced displacement. Analytic results show a possible exponential buildup of the inplane motion of the ribbon, ultimately limited by damping in the ribbon and spacecraft. The analysis indicates that the thermal lag time constant is fundamental for an increase in the antisymmetric mode period. Though there is good overall qualitative agreement with flight data, the numerical comparison of the ripple period is not as good as desired.

6. REFERENCES

1. R. W. Longman and J. A. Massart, "An Investigation of the Anomalous Attitude Motion of the ISEE-B Spacecraft," 1981.
2. J. V. Fedor, "Wire Antenna Motion Damper for IMP-I Spacecraft," X-732-73-293, October 1973.